DEPARTMENT OF AEROSPACE ENGINEERING

Faculty Name	:	**Dr.A.Arun Negemiya, ASP/ Aero**	Academic Year	:	**2024-2025 (Even)**
Year & Branch	:	**III AEROSPACE**	Semester	:	**VI**
Course	:	**19ASB304 - Computational Fluid Dynamics for Aerospace Application**			

UNIT II - DISCRETIZATION

Boundary Layer Theory and Its Importance

Boundary Layer Equations and Methods of Solution-Implicit Time Dependent Methods for Inviscid and Viscous Compressible Flows-Concept of Numerical Dissipation- Stability Properties of Explicit and Implicit Methods-Conservative Upwind Discretization for Hyperbolic Systems-Further Advantages of Upwind Differencing

Boundary Layer Equations and Methods of Solution

Prandtl made an important contribution to the calculation of a specific type of flow for which the Reynolds number is very large. The Reynolds number has the form of a non-dimensional parameter

$$\mathrm{Re} = \frac{LV}{\nu} = \frac{\rho L V}{\mu}$$

Where L is a characteristic length, usually the length of the considered body, V is the velocity of the flow where it is well-defined and undisturbed. The kinematic and dynamic viscosity is denoted by v and μ, respectively. The density of the fluid is ρ. The Reynolds number is the ratio of inertia to friction forces following the principle of similarity

$$\mathrm{Re} = \frac{\rho u \partial u/\partial x}{\mu \partial^2 u/\partial x^2} \equiv \frac{\text{inertia force}}{\text{friction force}}$$

The velocity u at some point in the velocity field is proportional to the free stream velocity V. The velocity gradient $\partial u/\partial x$ is proportional to V/L and similarly $\partial^2 u/\partial x^2$ is proportional to V/L^2. Hence the ratio, Eq. (2) yields

$$\mathrm{Re} = \frac{\rho V^2/L}{\mu V/\mathrm{d}^2} = \frac{\rho L V}{\mu}$$

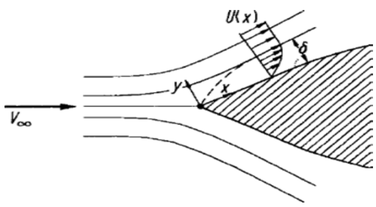

Figure 1:Boundary layer flow along a wall

Two flows are similar from the point of view of the relative importance of inertial and viscous effects if the Reynolds number is constant. Now the physical phenomenon of a flow with high Reynolds number is considered for the example of a cylindrical body shown in Fig. 1.

With the exception of the immediate neighborhood of the surface the flow velocity is comparable to the free stream velocity *V*. This flow region is nearly free of friction; it is a potential flow. Considering the region near the surface there is friction in the flow which means that the fluid is retarded until it adheres at the surface. The transition from zero velocity at the surface to the full magnitude at some distance from it takes place in a very thin layer, the so-called 'boundary layer'. Its thickness is δ, which is a function of the downstream coordinate x and is assumed to be very small compared to the length of the body L. In the normal direction y inside the thin layer it is clear that the gradient $\partial u/\partial y$ is very large compared to gradients in the stream wise direction $\partial u/\partial x$. Although the viscosity was meant to be very small in this flow the shear stress $\tau = \mu(\partial u/\partial y)$ may assume large values. Outside the boundary layer the velocity gradients are negligibly small and the influence of the viscosity is unimportant. The flow is frictionless and potential.

The above assumptions are now used to simplify the Navier–Stokes equations for steady two-dimensional, laminar and incompressible flows, resulting from the non-conservation form by a formal procedure. Including the continuity equation they have the following dimensional form in Cartesian coordinates

$$\bar{u}\frac{\partial \bar{u}}{\partial \bar{x}} + \bar{v}\frac{\partial \bar{u}}{\partial \bar{y}} = -\frac{1}{\bar{\rho}}\frac{\partial \bar{p}}{\partial \bar{x}} + \frac{\bar{\mu}}{\bar{\rho}}\left(\frac{\partial^2 \bar{u}}{\partial \bar{x}^2} + \frac{\partial^2 \bar{u}}{\partial \bar{y}^2}\right) \quad \text{----------------------------- 4}$$

$$\bar{u}\frac{\partial \bar{v}}{\partial \bar{x}} + \bar{v}\frac{\partial \bar{v}}{\partial \bar{y}} = -\frac{1}{\bar{\rho}}\frac{\partial \bar{p}}{\partial \bar{y}} + \frac{\bar{\mu}}{\bar{\rho}}\left(\frac{\partial^2 \bar{v}}{\partial \bar{x}^2} + \frac{\partial^2 \bar{v}}{\partial \bar{y}^2}\right) \quad \text{---------------------------- 5}$$

$$\frac{\partial \bar{u}}{\partial \bar{x}} + \frac{\partial \bar{v}}{\partial \bar{y}} = 0 \quad \text{-------------------- 6}$$

Here the velocity components ¯*u* and ¯*v* are directed towards the downstream ¯*x* and the normal ¯*y*-direction, respectively. The static pressure is denoted by ¯*p*, ¯ρ is the density and ¯μ is the dynamic viscosity of the fluid.

For convenience, this set of second order differential equations is non-dimensionalized which involves the Reynolds number necessary for the following reduction of the equations. The prescriptions for non dimensionalization are:

$$u = \frac{\bar{u}}{V} = 0(1)$$
$$v = \frac{\bar{v}}{V} = 0(\varepsilon)$$
$$p = \frac{\bar{p}}{\bar{\rho}V^2} = 0(1) \qquad \mathrm{Re} = \frac{\bar{\rho}LV}{\bar{\mu}} = 0\left(\frac{1}{\varepsilon^2}\right)$$
$$x = \frac{\bar{x}}{L} = 0(1)$$
$$y = \frac{\bar{y}}{L} = 0(\varepsilon)$$

----------------- 7

V is the dimensional free stream velocity and the pressure is non-dimensionalized by twice the dynamic pressure,

$$\bar{q} = \tfrac{1}{2}\bar{\rho}V^2$$

Using these definitions, Eqs. (4), (5) and (6) become:

$$u\frac{\partial u}{\partial x} + v\frac{\partial u}{\partial y} = -\frac{\partial p}{\partial x} + \frac{1}{\mathrm{Re}}\left(\frac{\partial^2 u}{\partial x^2} + \frac{\partial^2 u}{\partial y^2}\right)$$
$$(1)\frac{(1)}{(1)}(\varepsilon)\frac{(1)}{(\varepsilon)} \qquad (1) \qquad (\varepsilon^2)\left(\frac{(1)}{(1)} \qquad \frac{(1)}{(\varepsilon^2)}\right)$$

--------------------- 8

$$u\frac{\partial v}{\partial x} + v\frac{\partial v}{\partial y} = -\frac{\partial p}{\partial y} + \frac{1}{\mathrm{Re}}\left(\frac{\partial^2 v}{\partial x^2} + \frac{\partial^2 v}{\partial y^2}\right)$$
$$(1)\frac{(\varepsilon)}{(1)} \quad (\varepsilon)\frac{(\varepsilon)}{(\varepsilon)} \qquad (\varepsilon^2)\left(\frac{(\varepsilon)}{(1)} \qquad \frac{(\varepsilon)}{(\varepsilon^2)}\right)$$

--------------- 9

$$\frac{\partial u}{\partial x} + \frac{\partial v}{\partial y} = 0$$
$$\frac{(1)}{(1)} \quad \frac{(\varepsilon)}{(\varepsilon)}$$

----------------------- 10

Now the question is, what order of magnitude do the dimensionless substitutions Eqs. (8.7) have? As stated above, the boundary layer thickness δ is very small, so is the distance *y* compared to the length of the body *L*. Consequently *y* is of the order ε which describes a value much smaller than 1. The *u*-velocity component can reach the maximum value of *V*, therefore it is of the order 1. But the *v*-velocity component also has to be of the order ε as can be seen from the continuity equation, Eq. (8.10).If the derivative $\partial u/\partial x$ is of the order 1 because *x* becomes, at its maximum, the length *L*, then the second term in the continuity equation $\partial v/\partial y$ has also to be of the order 1. Consequently, *v* is not greater than ε. Now, with these assumptions the order of magnitude analysis can be done. It follows from the first equation of motion, Eq. (8.8), that the viscous forces in the boundary layer can become of the same order of magnitude as the inertia forces only if the Reynolds number is of the order of $1/\varepsilon^2$. The equation of continuity remains unaltered for very large Reynolds numbers.

The equation of continuity remains unaltered for very large Reynolds numbers. The downstream momentum equations can be reduced by the second derivative of the *u*-velocity component $\partial^2 u/\partial x^2$ and multiplied by 1/Re because it has the smallest order of magnitude in this equation. It only holds that the forcing function term ($-dp/dx$) will not exceed the order of 1 to be in balance with the other remaining terms.

All terms of the normal momentum equation, Eq. (8.9), are of a smaller magnitude than those of Eq. (8.8). This equation can only be in balance if the pressure term is of the same order of magnitude. Therefore, this equation delivers the information of negligible pressure gradient in the normal direction, i.e.

$$\frac{\partial p}{\partial y} = 0(\varepsilon)$$

The meaning of this result is that the pressure is practically constant; it is 'impressed' on the boundary layer by the outer flow. Therefore, the pressure *p* is only a function of x.

The derivation of Eq. (8.8) at the outer edge of the boundary layer gives, if the Inviscid velocity distribution $U(x) = \bar{u}(x)/V$ is known:

$$U\frac{dU}{dx} = -\frac{1}{\rho}\frac{d\rho}{dx} \qquad \text{-----------------}$$

The other terms involving $\partial u/\partial y$ are zero since there remains no large velocity gradient. After integration of Eq. (8.12) the well-known Bernoulli equation is found:

$$p + \frac{1}{2}\rho U^2 = \text{const.}$$ -----------------------

Summing up , by the order of magnitude analysis the Navier–Stokes equations, Eqs. (8) and (9), and the continuity Eq. (10), have been simplified. They are known as 'Prandtl's boundary layer equations':

$$u\frac{\partial u}{\partial x} + v\frac{\partial u}{\partial y} = -\frac{\partial p}{\partial x} + \frac{1}{\text{Re}}\frac{\partial^2 u}{\partial y^2}$$ -----------11

$$\frac{\partial p}{\partial y} = 0$$ ------------------ 12

$$\frac{\partial u}{\partial x} + \frac{\partial v}{\partial y} = 0$$ ---------13

The boundary conditions are:
On the surface:

$$y = 0 \qquad u = 0, \qquad v = 0$$ ------14

On the outer edge of the boundary layer:

$$y = \delta = \frac{\bar{\delta}}{L} \qquad u = U(x)$$ -----------15

This set of equations is reduced by the unknown pressure *p*, which is, because of Bernoulli's equation, Eq. (8.13), a known value now, if only the inviscid velocity distribution at the surface *U*(*x*) is provided. It is still a coupled, non-linear, second order set of differential equations.

The order of magnitude analysis also described by Schlichting [6] is well suited to analyse the more complicated surface-oriented Navier–Stokes equations with additional surface curvature created Coriolis and centrifugal forces. At least the order of magnitude analysis gives an impression where the boundary layer equations and their more complicated extensions are situated in their level of approximation to the full Navier–Stokes equations. This overview will be given in the next section.

HIERARCHY OF THE BOUNDARY LAYER EQUATIONS

To develop a hierarchy of the fluid mechanical equations, the steady, compressible, laminar, two-dimensional Navier–Stokes equations should be written for the Euclidian space in a layer close to the surface. This will say that a coordinate system, which may be surface oriented for a better adaption to the flow problem considered, is related to the cartesian coordinate system. Both systems must be transferable from one to the other. The cartesian and the polar coordinate system, for example, are matched together following this demand of Euclidian space. In other words, the Jacobian matrix must exist.

If the Navier–Stokes equations can be formulated for such a surface-oriented coordinate system, they will contain many additional terms due to the surface curvature. These terms can be understood as Coriolis and centrifugal force terms caused by the change of the streamlines in downstream as well as in the cross flow direction depending on the curvature of the surface. Curvature-induced terms will have different orders of magnitude. Some are important and others can be neglected depending on the specific flow problems.

Now the question is to set the boundary layer equations including curvature terms in relation to Prandtl's boundary layer equations developed in the foregoing chapter.

A simple two-dimensional surface-oriented coordinate system is fixed on an airfoil-like contour sketched in Fig. 1. The relations between the new coordinate system and the cartesian one are:

$$x = \int_0^s \cos\theta(x)\, \mathrm{d}s - n\sin\theta(x) \qquad \text{-- 1}$$

$$y = \int_0^s \sin\theta(x)\, \mathrm{d}s + n\cos\theta(x) \qquad \text{-- 2}$$

The resultant set of differential equations due to the coordinate transformation consists of two equations of motion in the downstream direction *s* and the perpendicular direction *n*, the energy and the continuity equations.

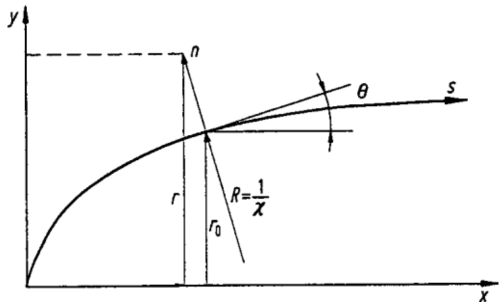

Fig. 1 Surface oriented coordinate system

Momentum equation in tangential direction:

$$\rho\left[u\frac{\partial u}{\partial s}+Hv\frac{\partial u}{\partial n}+\kappa uv\right]=-\frac{\partial p}{\partial s}+\frac{\partial}{\partial s}\left[\frac{4}{3}\frac{\mu}{H}\frac{\partial u}{\partial s}+\frac{4}{3}\frac{\kappa\mu v}{H}-\frac{2}{3}\mu\frac{\partial v}{\partial n}\right]$$
$$+H\frac{\partial}{\partial n}\left[\frac{\mu}{H}\frac{\partial v}{\partial s}+\mu\frac{\partial u}{\partial n}-\frac{\mu\kappa u}{H}\right]$$

----------------3

Momentum equation in normal direction:

$$\rho\left[u\frac{\partial v}{\partial s}+Hv\frac{\partial v}{\partial n}-\kappa u^2\right]=-H\frac{\partial p}{\partial n}+H\frac{\partial}{\partial n}\left[\frac{4}{3}\mu\frac{\partial v}{\partial n}-\frac{2}{3}\frac{\mu}{H}\frac{\partial u}{\partial s}-\frac{2}{3}\frac{\mu\kappa v}{H}\right]$$
$$+\frac{\partial}{\partial s}\frac{\mu}{H}\frac{\partial v}{\partial s}+\mu\frac{\partial u}{\partial n}-\frac{\mu\kappa u}{H}$$
$$+2\kappa\left[\mu\frac{\partial v}{\partial n}-\frac{\mu}{H}\frac{\partial u}{\partial s}-\frac{\mu\kappa v}{H}\right]$$

---------- 4

Energy equation:

$$c_p\rho\left[u\frac{\partial T}{\partial s}+Hv\frac{\partial T}{\partial n}\right]=u\frac{\partial p}{\partial s}+Hv\frac{\partial p}{\partial n}+\frac{\partial}{\partial s}\left[\lambda\frac{\partial T}{\partial s}\right]+H\frac{\partial}{\partial n}\left[\lambda\frac{\partial T}{\partial n}\right]$$
$$+H\frac{\mu}{2}\left\{\left[\frac{2}{H}\frac{\partial u}{\partial s}+2\frac{\kappa v}{H}\right]^2\right.$$
$$\left.+\left[2\frac{\partial v}{\partial n}\right]^2+2\left[\frac{1}{H}\frac{\partial v}{\partial s}+\frac{\partial u}{\partial n}-\frac{\kappa u}{H}\right]^2\right\}$$
$$-\frac{2}{3}H\mu\left[\frac{1}{H}\frac{\partial u}{\partial s}+\frac{\kappa v}{H}+\frac{\partial v}{\partial n}\right]^2$$

---------------- 5

Continuity equation:

$$\frac{\partial(\rho u)}{\partial s}+\frac{\partial(H\rho v)}{\partial n}=0$$

------------- 6

$$H=1+\kappa n=\frac{R+n}{R}$$

Here u and v are the velocity components in the tangential direction of the flow s and the normal direction n, respectively. The pressure is denoted by p, ρ is the density, μ and λ are the dynamic viscosity and the thermal heat conductivity, respectively. The curvature of the surface is involved in the geometrical coefficient *H*. This dimensional set of differential equations describes the laminar, compressible flow along arbitrary, two-dimensional curved surfaces.

Now these governing equations are analysed by predicting the order of magnitude of each term. As is usually done, the equations will be non-dimensionalized, the geometrical quantities by a characteristic length *L* and the flow properties by their free stream conditions denoted by subscript ∞. The order of magnitude of these quantities is defined as has been done in the case of a simple boundary layer without curvature in the preceding chapters.

$$s = \frac{\bar{s}}{L} = 0(1), \qquad n = \frac{n}{L} = 0(\varepsilon), \qquad \kappa = \bar{\kappa}L = 0(1)$$

$$H = 1 + \bar{\kappa}\bar{\eta} = 0(1), \qquad u = \frac{\bar{u}}{u_\infty} = 0(1), \qquad v = \frac{\bar{v}}{u_\infty} = 0(\varepsilon)$$

$$T = \frac{\bar{T}}{T_\infty} = 0(1) \qquad p = \frac{\bar{p}}{\rho_\infty u_\infty^2} = 0(1) \qquad \rho = \frac{\bar{\rho}}{\rho_\infty} = 0(1)$$

$$\mu = \frac{\bar{\mu}}{\mu_\infty} = 0(1) \qquad \lambda = \frac{\bar{\lambda}}{\lambda_\infty} = 0(1) \qquad c_p = \frac{\bar{c}_p}{c_{p\infty}} = 0(1)$$

$$Re = \frac{\rho_\infty u_\infty L}{\mu_\infty} = 0\left(\frac{1}{\varepsilon^2}\right) \qquad \text{Reynolds number}$$

$$Pr = \frac{c_{p\infty}\mu_\infty}{\lambda_\infty} = 0(1) \qquad \text{Prandtl number}$$

$$Ec = \frac{u_\infty^2}{c_{p\infty}T_\infty} = 0(1) \qquad \text{Eckert number}$$

------------------------ 7

It is to be mentioned that the radius of curvature *R* is not allowed to be much larger than the characteristic length *L*, otherwise κ would belong to another order of magnitude. The radius of curvature *R* is related to the curvature as follows

$$\kappa = \bar{\kappa}L = \frac{L}{R} \qquad \text{------------ 8}$$

When the radius *R* becomes very small compared to the length, *H* can exceed the order demanded above.

The combination of Eq. (7) with the governing equations, Eqs . (3), (4), (5) and (6), provides the order of magnitude of each term. A detailed development of the order of magnitude analysis applied to this set of equations seems not to be necessary here because in the preceding chapter an example was already presented. But in order to give an insight into the origin of the hierarchy of the boundary layer equations, the equations will be shown that retain terms only of the order 0(1) and 0(ε). The chosen equation is the tangential and normal momentum equation in dimensional unbarred form.

Order 0(1):

$$\rho\left(u\frac{\partial u}{\partial s}+Hv\frac{\partial u}{\partial n}\right)=-\frac{\partial p}{\partial s}+H\frac{\partial}{\partial n}\left(\mu\frac{\partial u}{\partial n}\right)$$ ----- 9

$$\frac{\partial p}{\partial n}=0$$ ------ 10

These equations, including the continuity equation, are called the 'first order boundary layer equations'. Curvature effects are included in the quantity *H* defined in Eq. (6). These equations become identical to Prandtl's boundary layer equations when the curvature goes to zero. Hence, Prandtl's equations are the lowest level of the hierarchy and therefore they should be called 'Zeroth order boundary layer equations'.

Now terms of the order 0(1) and 0(ε) are retained.

Order of magnitude 0(ε):

$$\rho\left(u\frac{\partial u}{\partial s}+Hv\frac{\partial u}{\partial n}+\kappa uv\right)=-\frac{\partial p}{\partial s}+H\frac{\partial}{\partial n}\left(\mu\frac{\partial u}{\partial n}\right)-\kappa\frac{\partial u}{\partial n}u+\kappa\mu\frac{\partial u}{\partial n}$$ ------8.29

$$\frac{\partial p}{\partial n}=\frac{\kappa\rho u^2}{H}$$ ----------------8.30

These equations show a significant extension of the foregoing ones. In Eq. (8.29) an additional centrifugal term κuv appears as well as dissipative terms due to curvature on the right-hand side; but the most important extension appears in the normal momentum equation, Eq. (8.30). The pressure gradient normal to the flow is no longer zero. Eq. (8.30) is an integral equation for the pressure which is no longer impressed on the boundary layer from the Inviscid flow. These equations are the so-called 'second order boundary layer equations' and take into account that, even in the outer Inviscid flow normal to the surface, there exist velocity gradients due to the streamline curvature. The outer edge of the boundary layer is matched to this gradient which is no longer equal to zero as the first order of boundary layer theory prescribes. Consequently terms of higher order than 0(ε) will be retained now. The result is summarized in Table 8.1.

A decisive development takes place proceeding from the second to the third-order set. The mathematical character of the equation changes from parabolic to elliptic. Elliptic differential equations are pure boundary value problems while parabolic equations are initial-boundary value problems. The latter can be solved by the so called ‘marching procedure’, but the former require the calculation of the entire flow field surrounded by the boundaries which implies a greater numerical effort.

The conclusion of this discussion is that a boundary layer theory of order higher than second order immediately leads to elliptic equations. This complicates the method of solution because the parabolic approach of the original idea of boundary layer theory no longer holds.

The subject of the following chapter will be to give an impression as to how transformations of the governing first-order boundary layer equations influence the solution techniques positively.

Table 8.1 Hierarchy of the boundary layer equations

Theory	Equation of motion		Energy equation
Navier–Stokes 5th order	Elliptic	Elliptic	Elliptic
Theory 4th order	Elliptic N–S	Parabolic	Elliptic
Theory 3rd order	Elliptic	Parabolic	Elliptic
Boundary layer theory 2nd order	Parabolic	Integral equation	Parabolic
Boundary layer theory 1st order	Parabolic	Constant	Parabolic
Boundary layer theory 0th order	Parabolic	Constant	Parabolic
Prandtl boundary layer equation			

Numerical Solution Method:

Choice of Discretization Model

To come to a numerical solution of a set of partial differential equations it is usual to replace the differential quotients by finite difference quotients taking into account that a truncation error of a certain order of magnitude will now be induced to the set of equations. By rearranging the finite difference equations a system of algebraic equations is obtained which can be solved by means of the known methods. The techniques of the discretization are detailed in

Chap.5. It is stated there that the choice of the computational discretization grid is important as it affects the truncation error, the stability and the consistency. The form of these grids and the solution methods to which they lead will be summarized briefly.

Parabolic equations as observed here have a first order differential in the marching direction. As the flow is not allowed to reverse, the values of each quantity at the last upstream grid line normal to the surface are known. If we consider a grid as shown in Fig. 8.3, where Δx and Δy are the step sizes in the tangential and normal direction to the surface, the known points are on the left-hand side and the unknown on the right. Also the boundary conditions at the wall are given. Therefore, it is easy to calculate the flow quantities at the point with the open circle using discretization models as already given in Chap. 5. Because of the direct calculation of only one point on the grid line, this is called an 'explicit method'. The explicit method causes strong restrictions in the choice of the downstream step size as will briefly be repeated later, so the scheme is slow.

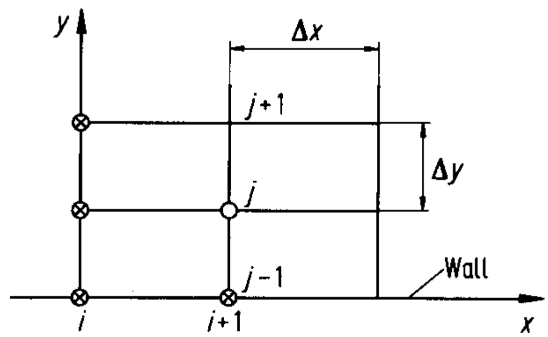

Grid for an explicit method

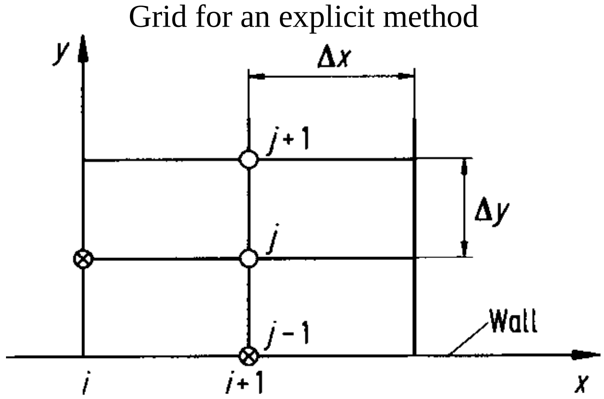

Grid for a fully implicit method

Figure 8.4 shows another extreme choice of a computational grid; the so-called 'fully implicit method'.

Only one known grid point from the preceding step is used, while on the actual one all points are unknown except the boundary values. That leads to an implicit form of the set of algebraic equations as will be shown later. This method is, concerning the choice of the step size, unconditionally stable but may lead to a poor accuracy. If there is no restriction on the step size in the downstream direction it becomes a fast calculation method which is desirable.

Now it is obviously possible to formulate something in between these extremes which will result in both a fast and accurate solution method. Figure 8.5 gives the computational mesh proposed by Crank–Nicholson [13] but in a more general form, so that the discretization methods described before are contained within it as special cases. Here, all points of the known and unknown grid lines are involved, but now the centre of discretization is located at the point $i + \lambda$. $\lambda = 1/2$ was originally proposed by Crank–Nicholson. Although the pure Crank–Nicholson scheme was described in detail in Part I, an example of a linear model equation is utilized to show its discrimination by the more generalized Crank–Nicholson scheme. In a following section the application to the two dimensional, rotational compressible boundary layer equations will be given.

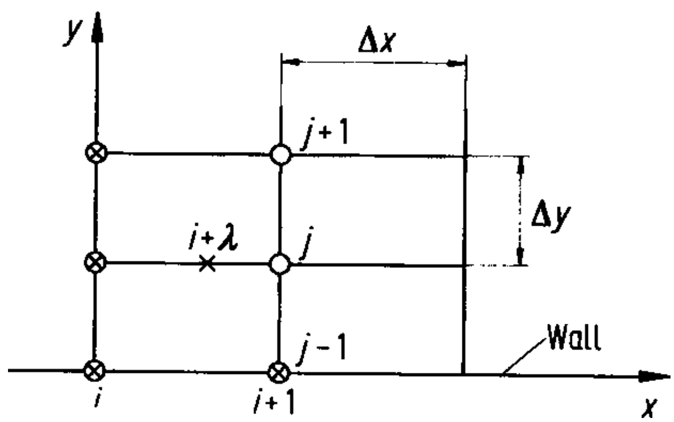

Grid for a generalized implicit method

Generalized Crank–Nicholson Scheme

This section is taken directly from Arina & Benocci [5]. In order to analyse the stability and accuracy of a generalization of the Crank–Nicholson scheme, it isconvenient to utilize the linear model Eq. (8.40),

$$\frac{\partial \phi}{\partial x} = a\frac{\partial^2 \phi}{\partial y^2} \qquad \text{------------8.40}$$

Equation (8.40) is discretized around the mesh point ($i + \lambda, j$), with λ ranging between 0 and 1. For λ = 0 an explicit scheme is recovered, while λ = 1 corresponds to the fully implicit case. If the grid is uniform, the *x*-derivative is approximated by the finite difference relation developed in Sect. 5.2.1.

$$\left(\frac{\partial \phi}{\partial x}\right)_{1+\lambda,j} = \frac{\phi_{i+1,j} - \phi_{i,j}}{\Delta x} + \left(\lambda - \frac{1}{2}\right) 0(\Delta x) + 0(\Delta x^2)$$

and the *y*-derivative is replaced by the weighted mean

$$\left(\frac{\partial^2 \phi}{\partial y^2}\right)_{i+\lambda,j} = \lambda \left(\frac{\partial^2 \phi}{\partial y^2}\right)_{i+1,j} + (1-\lambda)\left(\frac{\partial^2 \phi}{\partial y^2}\right)_{i,j}$$

Each second-order derivative is then replaced by the usual three-point centred finite difference relation:

$$\left(\frac{\partial^2 \phi}{\partial y^2}\right)_{i,j} = \frac{\phi_{i,j+1} - 2\phi_{i,j} + \phi_{i,j-1}}{\Delta y^2} + \left(\Delta y^2\right)$$

Substituting Eqs. (8.41, 8.42, 8.43) into equation (8.40), a linear difference equation is obtained

$$\frac{\phi_{i+1,j} - \phi_{i,j}}{\Delta x} = \frac{a}{\Delta y^2}\left[\lambda(\phi_{i+1,j+1} - 2\phi_{i+1,j} + \phi_{i+1,j-1}) + (1-\lambda)\left(\phi_{i,j+1} - 2\phi_{i,j} + \phi_{i,j-1}\right)\right]$$

which can be recast in the usual tridiagonal form

$$\left(-\lambda\frac{a\Delta x}{\Delta y^2}\right)\phi_{i+1,j-1} + \left(1 - 2\lambda\frac{a\Delta x}{\Delta y^2}\right)\phi_{i+1,j} + \left(\lambda\frac{a\Delta x}{\Delta y^2}\right)\phi_{i+1,j+1} = D_j$$

with *D*j a function of φ computed at station *i*.

To perform the von Neumann stability analysis it is useful to express the numerical solution as a Fourier series, and then verify that none of the harmonics is amplified with respect to the evolution coordinate *x*. This stability analysis is described in detail in Sect. 4.4; Part I, and is repeated here as a reminder. Hence putting

$$\phi_{i,j} = \rho^{i} e^{I\omega(j\Delta y)}$$

where *I* in the exponent is the unit complex number, and ρi is the amplification factor at level *i*, and then substituting inside Eq. (8.45), actualizing the indices in Eq. (8.46), we have

$$G = \frac{\rho^{i+1}}{\rho^{i}} = \frac{1 + 2a(1-\lambda)\frac{\Delta x}{\Delta y^2}[\cos(\omega\Delta y) - 1]}{1 + 2a\lambda\frac{\Delta x}{\Delta y^2}[\cos(\omega\Delta y) - 1]}$$

To have stability, $|G| \leq 1$ for all harmonics $\omega\Delta y$; this inequality together with Eq. (8.47), leads to the following stability condition for $0 \leq \lambda < ½$

$$C \leq \frac{1}{2(1-2\lambda)}$$

where $C = a\Delta x/\Delta y2$. For $1/2 \leq \lambda \leq 1$ no stability restriction is imposed on *C*. Hence the scheme presented is unconditionally stable for values of λ equal or larger than 1/2. In the case of the explicit scheme ($\lambda = 0$), there is a strong limitation to Δx if Δy is chosen rather small for accuracy requirements.

The consistency of the scheme can easily be verified expanding in Taylor series all other terms of Eq. (8.45) about the point (i+λ, j). The discretization error can be proved to be of 0(Δx, Δy2) if λ is not equal to 1 (Ref. [14]). The scheme is therefore second order accurate with respect to *y* and first-order with respect to *x*. To obtain second order accuracy with respect to *x*, λ should be taken equal to 1/2 (Crank–Nicholson scheme), or slightly different to 1/2 (e.g. = 1/2 + 0(Δx)). However, for practical, non-linear problems it is often necessary to increase λ in order to avoid non-linear instabilities. For instance, the full implicit scheme is often very stable, but leads to a worse accuracy.

Equation (8.40) is a linear partial differential equation employed as a model to demonstrate the widely used generalized implicit Crank–Nicholson solution code. Now this will be applied to the boundary layer Eqs. (8.31), (8.32) and (8.33) of Sect. 8.4.